Proc. NIPR Symp. Polar Meteorol. Glaciol., **5**, 9–23, 1992

TRANSPORT SIMULATION OF PASSIVE TRACERS FROM THE NORTHERN HEMISPHERE TO THE SOUTHERN HEMISPHERE

Koji YAMAZAKI[1] and Masaru CHIBA[1]

[1]*Meteorological Research Institute, 1-1, Nagamine, Tsukuba 305*

Abstract: In order to study the transport process of anthropogenic gases such as CO_2 and halocarbons, transport simulations are performed for passive tracers emitted from "Japan", "Europe", "North America" and "Amazon" regions. Three-dimensional wind data simulated by the Meteorological Research Institute Global Spectral Model with rhomboidal 24 truncation and 23 levels (MRI-GSPM-R24L23) are used. At each source grid point, one unit of tracer is emitted per day into the lowest model layer throughout the experiment. The starting time is December 1 and the calculation continues until mid-October of the next year.

It is found that equatorward transport from the NH source regions takes place mainly around the Siberian High and Mexican High in winter. Large gradients (tracer front) formed near the equator at low levels in all the NH cases. In the SH, tracer density increases with height in the troposphere in all cases. The above features are related to the inter-hemispheric transport. From the NH, tracers spread into the equator through the lower layer, move upward over the equator and are transported through the upper troposphere into the SH. The above results imply that transport is accounted for the observed latitudinal and vertical distribution of CO_2 and halocarbons, in addition to source/sink effect.

Upward bulges are found in the tropical lower stratosphere and the large vertical gradients in the lower stratosphere of the extratropics, indicating that transport from the troposphere to the stratosphere takes place through the tropical tropopause. In all the NH cases, in particular during the summer of case "Japan", a secondary tracer front is formed at about 40°N.

1. Introduction

Atmospheric carbon dioxide (CO_2) concentration is increasing globally mainly due to anthropogenic emission of fossil fuels and partly due to biomass burning. Also, concentrations of halocarbons (CCl_2F_2, CCl_3F etc.) are increasing globally due to anthropogenic emission. The latitudinal distributions of these gases at the surface show large gradients near the equator. Clear gaps are occasionally observed across the ITCZ (Intertropical Convergence Zone) and/or SPCZ (South Pacific Convergence Zone). For instance, see KEELING *et al.* (1984), KOMHYR *et al.* (1985), TANAKA *et al.* (1987) and AOKI (1988) for CO_2; HIROTA *et al.* (1985) and MAKINO (1988) for halocarbons. Transport seems to contribute to producing this latitudinal distribution.

Anthropogenic sources of CO_2 and halocarbons are mainly located in the Northern Hemisphere (NH). Nevertheless, concentrations of CO_2 and halocarbons are increasing even in the Southern Hemisphere (SH). In the SH, vertical distributions of CO_2 through the middle and upper troposphere show lower concentrations at lower altitudes throughout most of the year (PEARMAN and GARRATT, 1973; PEARMAN and BEARDSMORE, 1984; NAKAZAWA *et al.*, 1990). This vertical distribution is opposite to that in the NH where the source is located at the surface. One possible reason for this vertical profile in the SH is an oceanic CO_2 sink in middle latitudes. Another is the upper tropospheric meridional transport of NH air into the SH. For halocarbons, the vertical distribution is quite uniform over Antarctica (HIROTA *et al.*, 1984, 1986; MAKINO, 1988), while it gradually decreases with height in the NH troposphere (WMO, 1985). For halocarbons, the sink effect makes a negligible contribution to the distribution in the SH.

To investigate the global transport of anthropogenic gases, we have started a series of numerical simulations of tracer gas transport. As a first step, this paper presents the results of global and long-term simulation of *passive* tracers emitted from three regions in the NH and Amazon region. "*Passive*" means that tracers move with air and do not affect the circulation. Moreover, no source/sink term is considered in this study. This work is to clarify the role of large-scale transport for the global distribution of anthropogenic gases. Our main objective is to show how tracers are transported from the NH to the SH.

2. Model and Experiments

2.1. *Model*

The model used in this study is a primitive equation General Circulation Model in $\sigma(P/P_S)$ coordinate with 23 levels in the vertical extending from the surface to approximately 70 km in the middle mesosphere. In the horizontal the model uses the spectral transform method with a rhomboidal 24 truncation (R24). The associated Gaussian grid has 80 points in longitude with a spacing of 4.5 degrees and 62 points in latitude with an approximate spacing of 2.95 degrees.

The detalis of the model are given in CHIBA *et al.* (1986) and references therein except for the schemes of radiation, Rayleigh damping and horizontal advection of water vapor, which are different from CHIBA *et al.* (1986) and are described in SHIBATA and CHIBA (1990). Climatology of the R13L23 version is found in SHIBATA and CHIBA (1990).

The model was integrated for more than one year starting from November 1. The initial conditions for the model were taken from the Japan Meteorological Agency (JMA) analysis for 00Z of November 1, 1984. The simulated 12-hourly fields were stored on magnetic tape. The stored data were used for the transport calculation of passive tracers.

2.2. *Method and experiments*

In these experiments, a continuous source of tracer gas is placed over a certain region. Experiments are done for four source regions as shown in Fig. 1. Exact locations of the source points and the numbers of grids are shown in Table 1 for each case. At each source grid point, one unit of tracer is emitted per day into the lowest

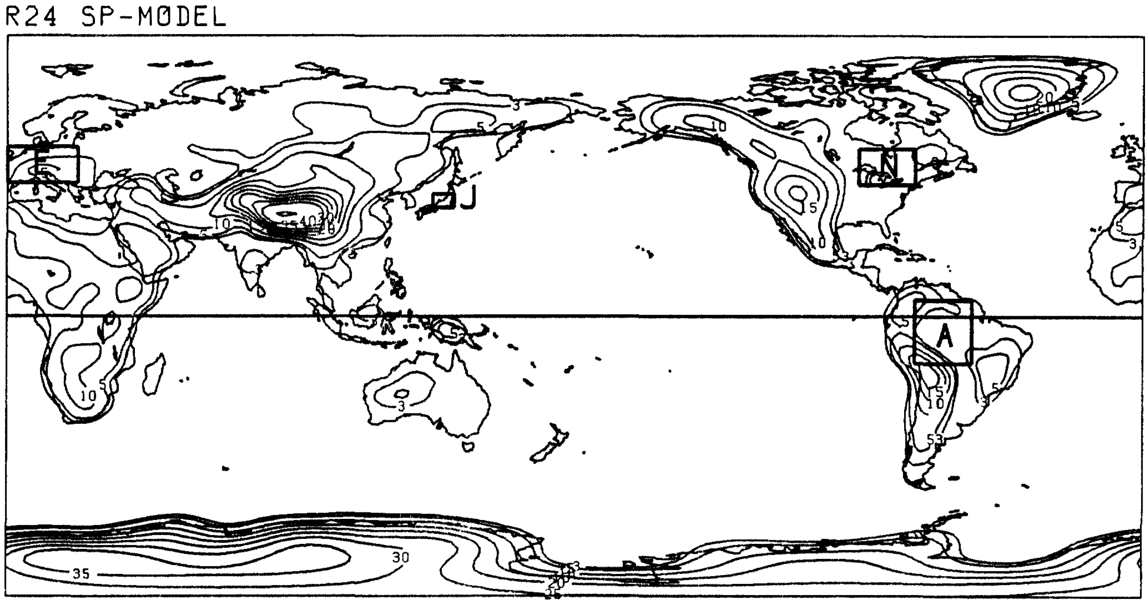

*Fig. 1. Topography used in the MRI-GSPM-R24 and source regions of transport simulation. Unit of topography is 10 m and contour interval is 500 m. The 300 m contour is also drawn. Thick rectangles denote source regions. **J** stands for case "Japan", **E** for "Europe", **N** for "North America" and **A** for "Amazon".*

Table 1. Source region and number of grids.

Case	Source region	Number of grids
Japan	135°E–144°E; 33°N–39°N	4 points
Europe	0°E–22.5°E; 42°N–57°N	30 points
North America	270°E–292.5°E; 42°N–57°N	25 points
Amazon	288°E–310.5°E; 15.9°S–7.3°N	40 points

model layer throughout the experiment. The depth of the lowest layer is about 20 hPa. The change of tracer density is calculated using the simulated wind data mentioned in the previous subsection. The starting time of the transport calculation is 00 UTC 1 December, discarding the first month when the flow is in a transient stage towards model's climate. The calculations were continued until mid-October of the next year.

The 3-dimensional semi-Lagrangian scheme (for the 2-dimensional scheme, see WILLIAMSON and RASCH, 1989 and references therein) is used for tracer transport, assuming that the tracers move along with the air parcel. Twelve-hourly simulated wind data were linearly interpolated to hourly data, and the scheme is applied to these hourly data. The time step for transport calculation is one hour. The 2-dimensional semi-Lagrangian scheme is used for water vapor transport in the Canadian operational numerical weather forecasting model (RITCHIE, 1987 and references therein) and also in the MRI-GSPM. In the semi-Lagrangian scheme, the density at a certain grid point is calculated as follows: The point where the air was located one time-step earlier is calculated, and the density at that backward point obtained by spacewise interpolation. The density at the grid point is set equal to that at the backward point. The scheme works well even when large density gradients exist, and there is no limitation on the time step to prevent numerical instabilities. Moreover, the scheme adopted in the current transport calculation preserves the tracer distribution shape well. In the present experiment, large gradients of tracer density form near the source region in the vertical as well as horizontal at an early stage. Therefore, the 3-dimensional semi-Lagrangian scheme seems to be appropriate to this experiment compared with a conventional advection scheme. On the other hand, the scheme does not guarantee conservation of total tracer mass, while the conventional scheme does.

In this experiment, no adjustment for total tracer mass conservation is applied. Subgrid-scale diffusion is not included in the transport calculation. Therefore, the present results are purely due to the grid-scale circulation transport.

3. Short-term Transport

In this section, characteristics of short-term transport, *i.e.*, during the first month,

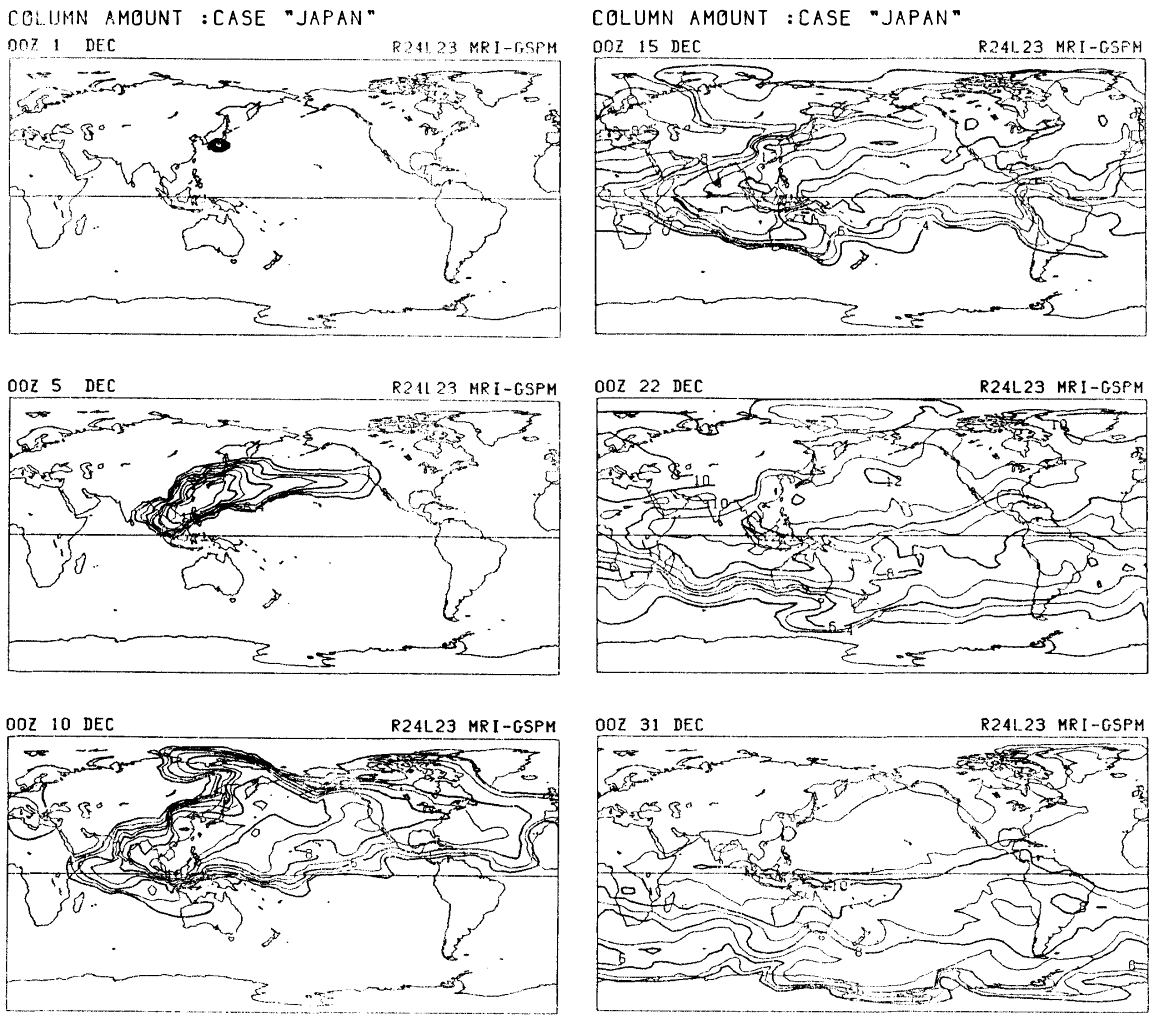

Fig. 2. Horizontal distribution of total column amount of tracers for selected dates during the first month for case "Japan". Effective date is shown on the top left corner of each panel. Contours are drawn with a logarithmic scale. Contour interval is 1. Contours less than 4 are not drawn.

are described.

3.1. Case "Japan"

Figure 2 shows the horizontal distribution of total column amount of tracers emitted from the Japan region during the first month. This figure and the following figures are plotted on a logarithmic scale: a difference of one in the figures means 10 times difference of the actual amount.

Part of tracers are moved eastward by the mid-tropospheric westerlies. The tracers spread into the NH within about 3 weeks. At low level, there is a strong

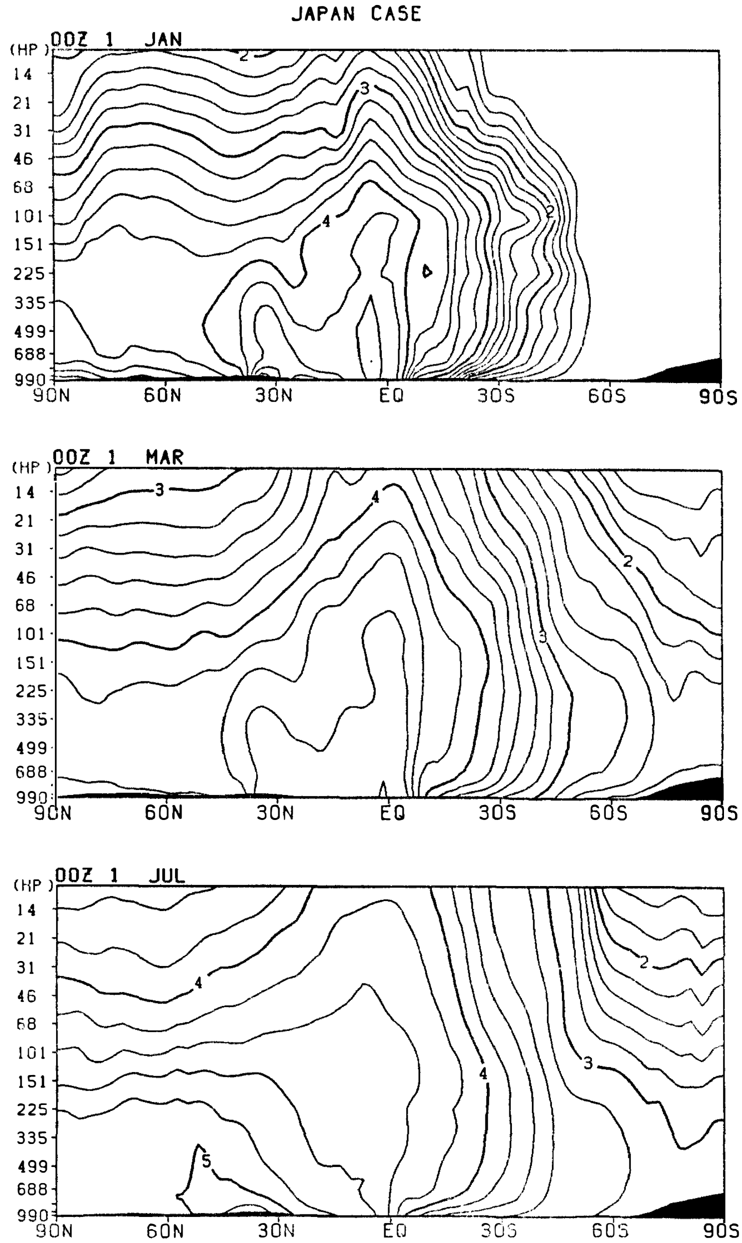

Fig. 3. Latitude-height cross section of zonal mean tracer density after one, three and seven months for case "Japan". Effective date is shown on the top left of each panel. Contours are logarithmic scale. Contour interval is 0.2. Contours less than 1.2 are not drawn.

equatorward flow southeast of the Siberian High. Another part moves southwestward following this near-surface flow around the Siberian High and reaches the tropical Indian Ocean within 2 weeks. Eastward and southwestward transport from Japan take place alternately, associated with the passage of cyclones. Tracers are transported into the SH over the Indian Ocean by the cross-equatorial flow near the surface. At the same time, tracers move upward near the equator, then turn eastward.

The top panel of Fig. 3 shows the latitude-height cross section of tracer density after one month on a logarithmic scale. Toward the equator, the tracers move near the surface. Near the equator upward motion is noticeable. These features can be clearly seen in the figure. At 20–30°N the low density region intrudes from above in the upper troposphere, which corresponds to the downward branch of the zonal-mean Hadley cell. Locally, this low density seems to be caused by an intrusion of stratospheric air through a tropopause gap. In the middle and upper troposphere, to the north of the source region, the density is quite uniform. The density in the Arctic region is low near the surface, which implies that the contribution to Arctic Haze from Japan is less important.

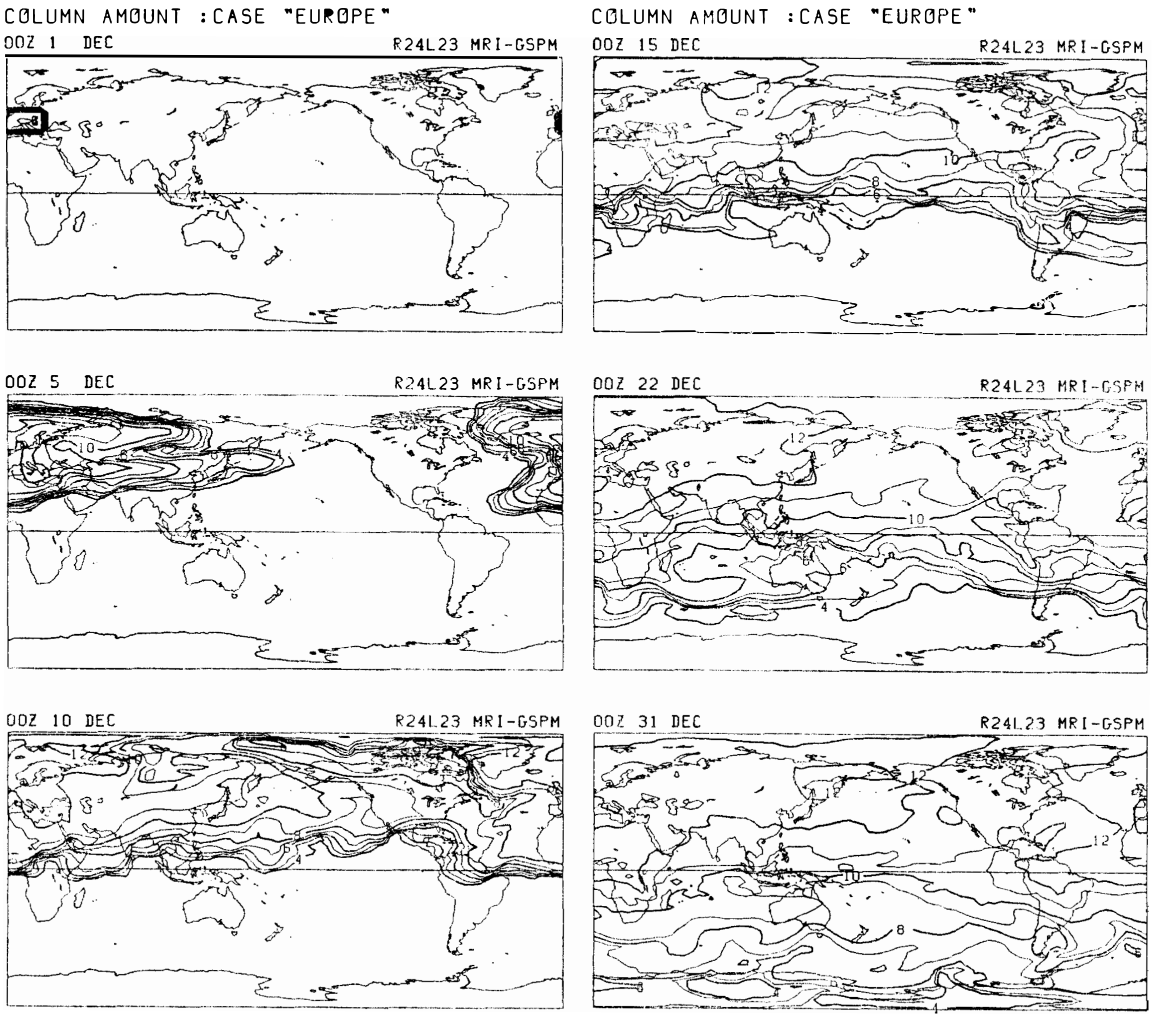

Fig. 4. Same as in Fig. 2 except for case "Europe".

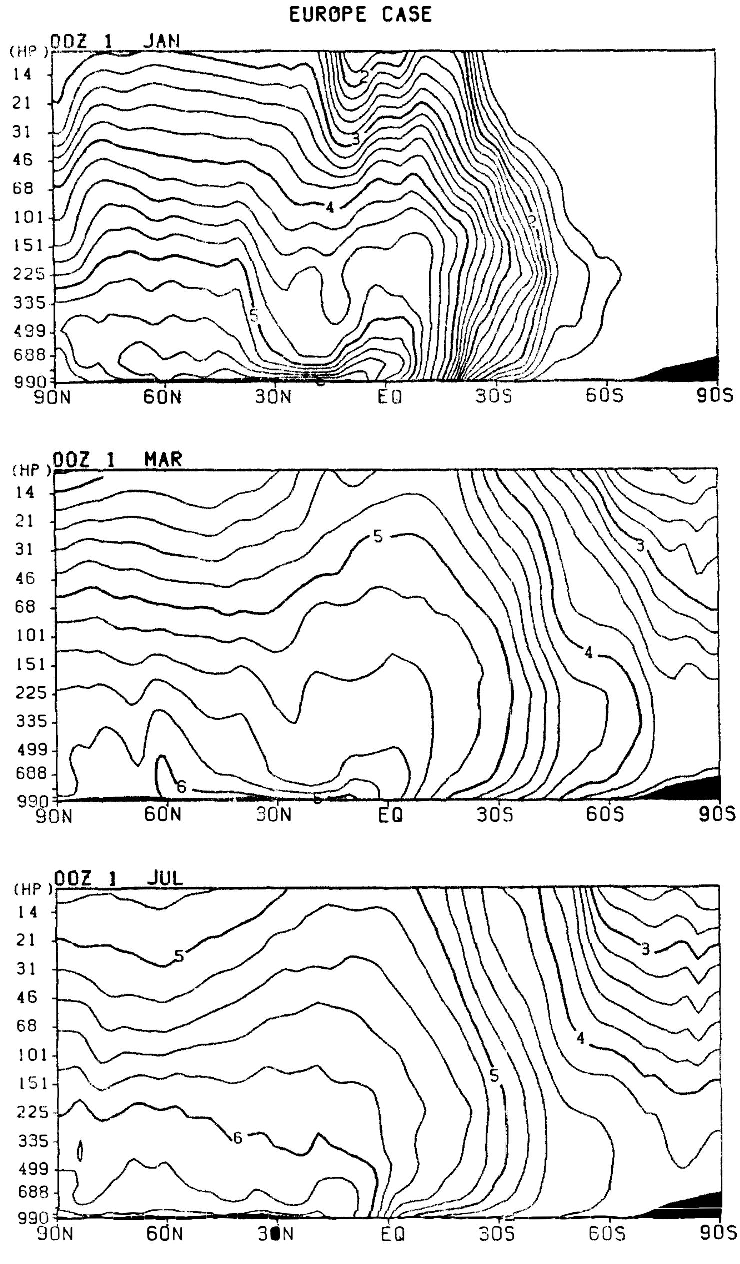

Fig. 5. Same as in Fig. 3 except for case "Europe".

3.2. Case "Europe"

Part of tracers are transported into the Arctic region (Fig. 4), which is different from case "Japan". Most move eastward; within 2–3 weeks tracers spread in the NH. An intrusion to the SH occurs, mainly over the eastern Pacific and Indian Oceans, after 2–3 weeks. After crossing the equator, southwestward movement turns into southeastward movement. At the same time, tracers move upward near the equator. The latitude-height cross section clearly shows these features (top panel of Fig. 5).

3.3. Case "North America"

Part of tracers are transported toward the Arctic (Fig. 6). Most tracers move

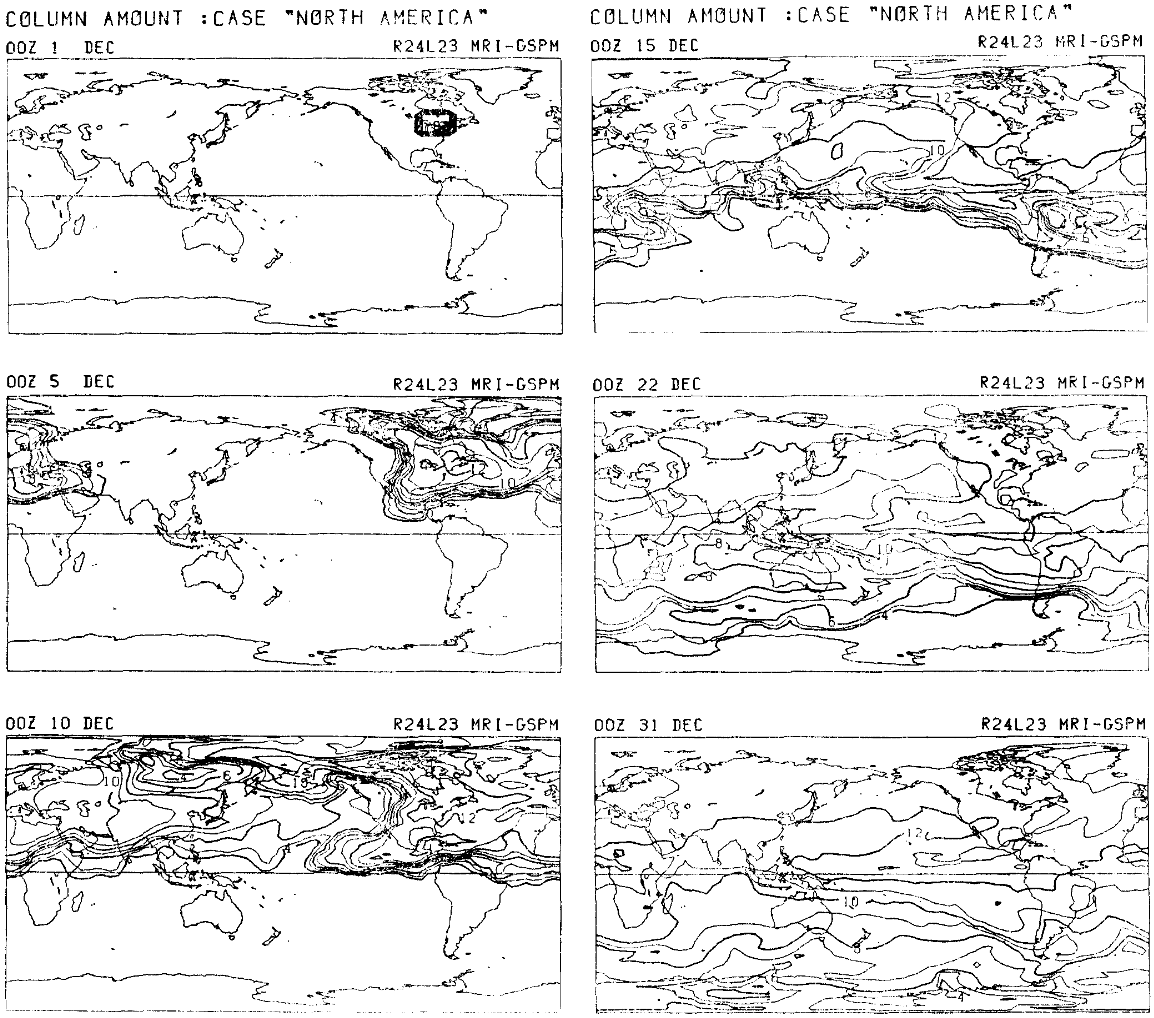

Fig. 6. Same as in Fig. 2 except for case "North America".

eastward and spread in the NH within 2–3 weeks. Part are transported southwestward toward the equator along the periphery of the Mexican High. Over the equatorial eastern Pacific, tracers intrude into the Southern Hemisphere accompanying upward motion and turn southeastward. These features are similar to those in case "Japan". After one month, as seen also in the top panel of Fig. 7, a high density region is found in the Arctic troposphere. Both this case and case "Europe" show large transport into the Arctic Haze region (HOFF, 1988; HEINTZENBERG, 1989).

3.4. Case "Amazon"

Figure 8 shows the horizontal distribution of total column amount of tracers emitted from the Amazon region during the first month. There are three main transport routes. The first is near-surface westward transport along the equator. The second is upward and southward transport in the SH. When tracers reach about 30°S, they are transported eastward by the subtropical westerly jet. The third is nearly a mirror image of the second around the equator. After one month, tracers spread within the tropical and subtropical regions in both hemispheres. Transport

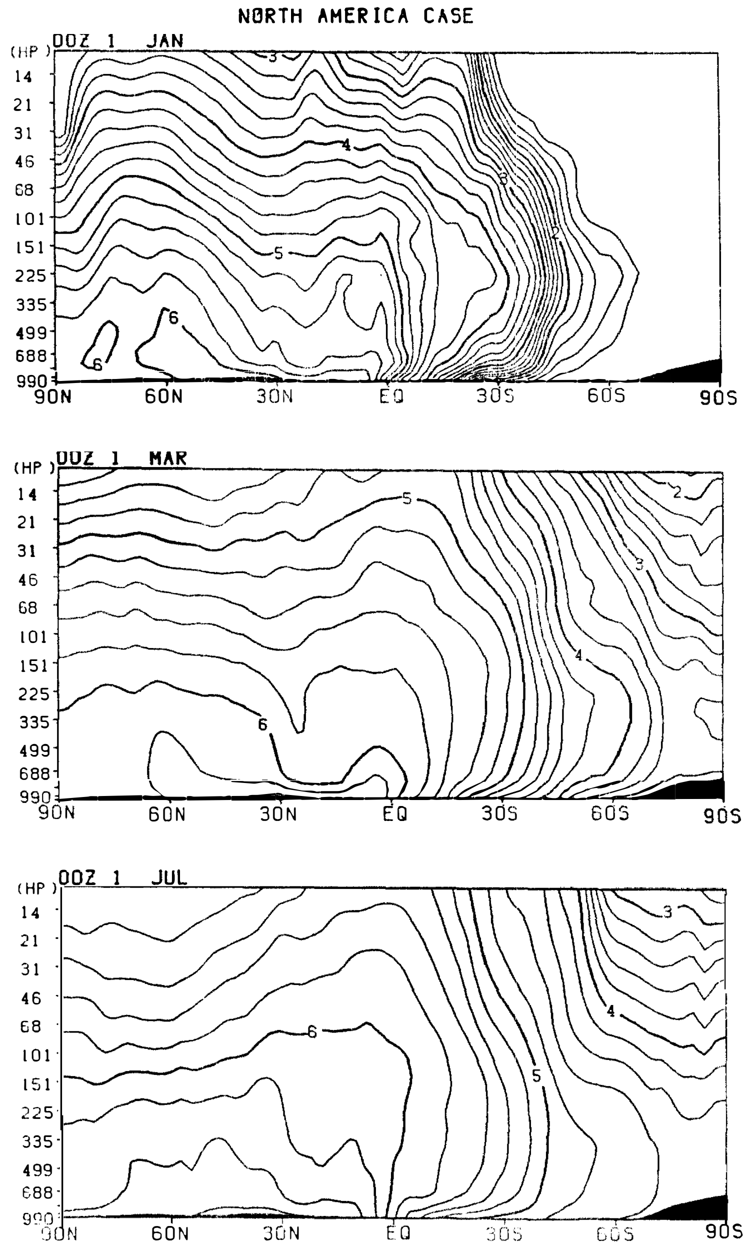

Fig. 7. Same as in Fig. 3 except for case "North America".

to the SH is faster than that to the NH. This case can be considered as a transport simulation of biomass burning (HEINTZENBERG and BIGG, 1990).

The top panel of Fig. 9 shows the latitude-height cross section of tracer density after one month. In this case, it is interesting to note that the highest density in the zonal mean field appears in the upper tropical troposphere, and not near the surface as in the other cases.

4. Long-term Transport

4.1. Latitude-height cross section

Figures 6–9 show the latitude-height cross sections of zonal mean tracer density

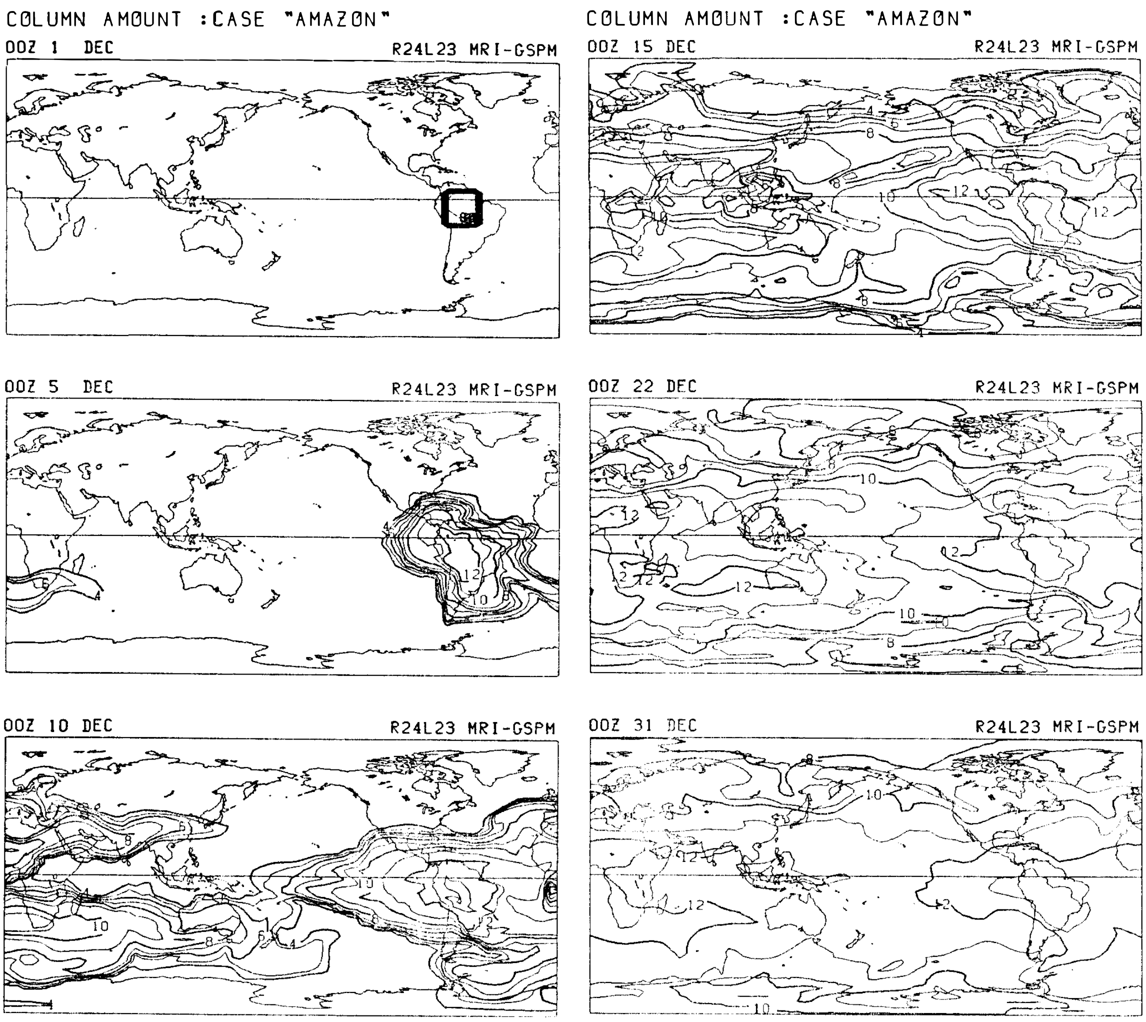

Fig. 8. Same as in Fig. 2 except for case "Amazon".

after one, three and seven months from top to bottom, respectively, for each case. In all cases, an upward bulge of the high density region is noticeable in the tropical lower stratosphere. This indicates that transport from the troposphere to the stratosphere takes place through the tropical tropopause. In particular, case "Amazon" clearly shows this transport process.

In all cases, the density in the Antarctic stratosphere is extremely low. The calculation continued until October and even in October, this feature is still noticeable (figures not shown). This is because the strong polar vortex in the SH during early winter to spring prevents transport from mid-latitude to the polar region (YAMAZAKI, 1986, 1987, 1989). If the calculation were continued until the austral summer, density in the Antarctic stratosphere would be expected to increase, associated with breakdown of the polar vortex.

In all the NH source cases ("Japan", "Europe" and "North America"), large latitudinal gradients (tracer fronts) form near the equator at low levels. In the horizontal distribution, the tracer front is found along the ITCZ (Intertropical Convergence Zone). These features are observed in the CO_2 concentration (TANAKA

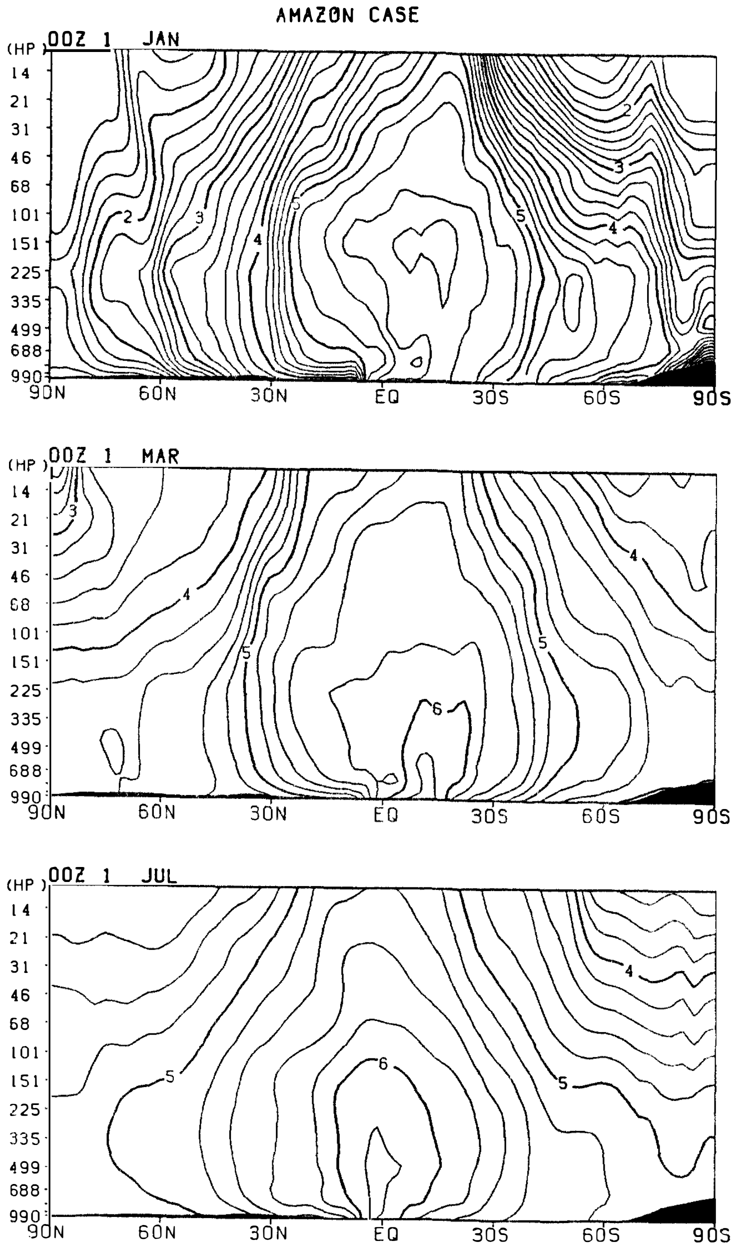

Fig. 9. Same as in Fig. 3 except for case "Amazon".

et al., 1987). On the other hand, a tracer front is not found in the tropical middle-to-upper troposphere. Instead, in the middle-to-upper troposphere, moderate gradients are found in subtropical latitudes.

In middle latitudes of the SH, density in the upper and middle troposphere is higher than that at the lower level: density increases with height in the troposphere. This vertical profile is observed in the CO_2 concentration in the SH. These features can be seen in both hemispheres in the case "Amazon". This pattern is formed due to upward transport near the equator. Transport from the tropics dominates in the upper troposphere. When tracers move across the equator, they are adevected upward near the equator and transported into the other hemisphere through the upper troposphere.

4.2. Variation of zonal mean column amount

Figure 10 shows the time-latitude plot of zonal mean column amount for case "Japan". This figure is plotted with a normal scale and not with a logarithmic scale. Large gradients (tracer fronts) persist near the equator, accompanying a slight latitudinal shift with season. The tropical tracer front is located at about 5°S during winter to spring and shifts to around 5°N in summer and fall with decreasing gradients. The seasonal shift of the tropical tracer front is associated with the seasonal shift of ITCZ. During winter to early spring, the maximum in column amount is located just north of the tropical tracer front and not over the source region. This is partly because a deep and dense layer is formed in the tropics, while dense layer is shallow in the subtropics (see Fig. 3).

In summer, a secondary tracer front is formed around 30–40°N; the maximum is found at about 45°N. During summer, tracers move northeastward along the periphery of the Pacific High and tend to stagnate over the North Pacific and Alaska (Fig. 11). Also, a deep and dense layer forms there (see also Fig. 3). In fall, the mid-latitude tracer front moves equatorward and merges with the tropical tracer front.

Other cases are omitted to save space, but are summarized briefly. The tropical front is found in all the NH cases. In the other NH cases, the weak mid-latitude tracer

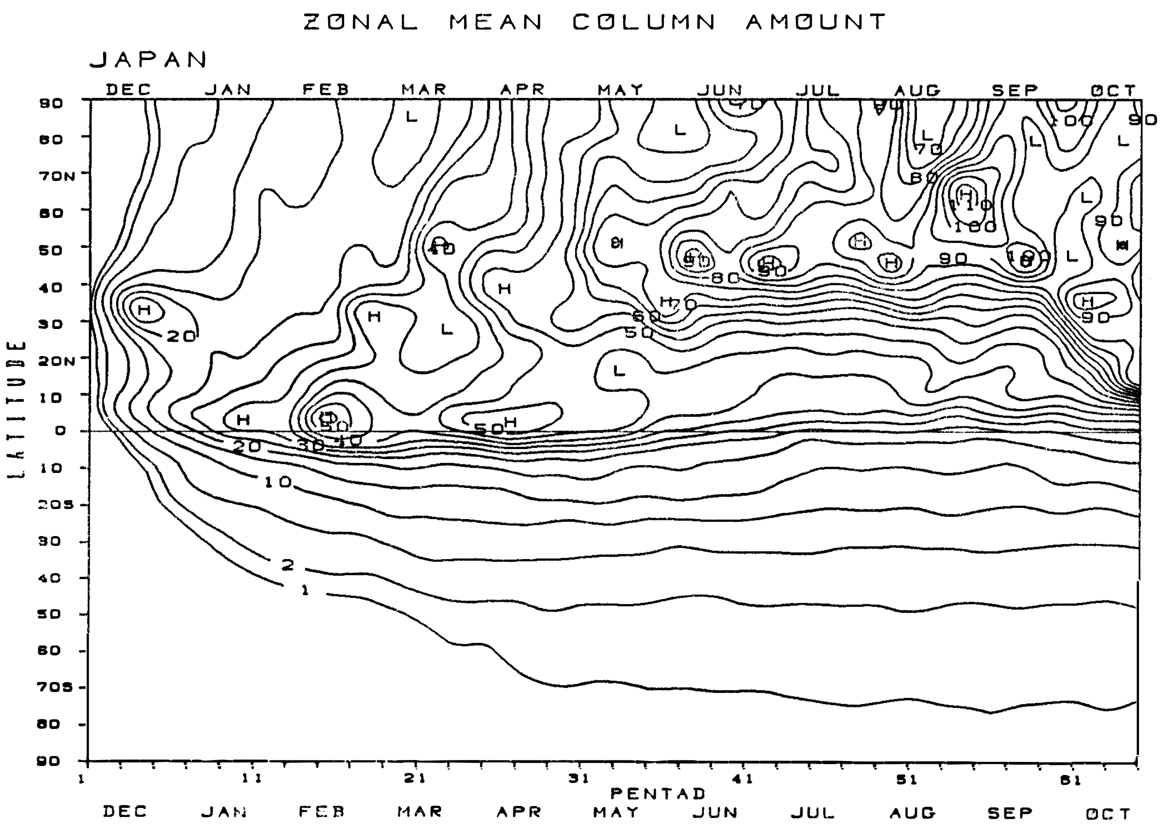

Fig. 10. Time-latitude plot of zonal mean total column amount of tracers for case "Japan". Contours are drawn with a normal scale. Contour interval is 5. Contours for 1 and 2 are also drawn. The figure is drawn based on 5-day (pentad) mean data.

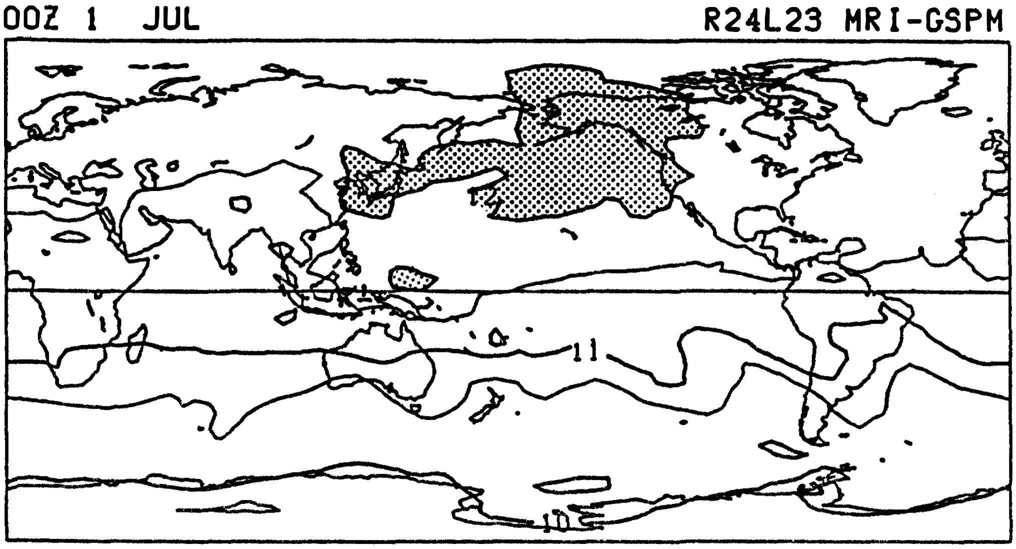

Fig. 11. Horizontal distribution of total column amount of tracers for 1 July for case "Japan". Contours are drawn with a logarithmic scale. Contour interval is 0.5. Regions greater than 12 are shaded.

front is found throughout the year. In case "Amazon", diffusion into the SH is large during winter and spring. The spring maximum of elemental carbon, which is considered to be due to biomass burning in low latitudes, observed at Cape Grim, Tasmania, might be related to the annual variation of transport (HEINTZENBERG and BIGG, 1990).

5. Summary and Discussion

Transport simulations have been performed for passive tracers emitted from "Japan", "Europe", "North America" and "Amazon". The main results obtained in the present study are as follows:

(1) In winter, equatorward transport from the NH source regions takes place mainly associated with the low level monsoon flow (*i.e.*, around the Siberian High and Mexican High).

(2) Large gradients (tracer front) are formed near the equator at low levels in all NH cases.

(3) In the SH, tracer density increases with height in the troposphere in all cases.

The above three items are related to the inter-hemispheric transport. From the NH, tracers spread into the equator through the lower layer, move upward over the equator and are transported through the upper troposphere into the SH. The above results imply that transport is accounted for the observed latitudinal and vertical distribution of CO_2 and halocarbons, in addition to source/sink effect.

(4) Upward bulges are found in the tropical lower stratosphere, and large vertical gradients in the lower stratosphere of the extratropics.

This is an indication that transport from the troposphere to the stratosphere takes place through the tropical tropopause.

(5) In all the NH cases, in particular during the summer of case "Japan", a secondary

tracer front is formed at about 40°N

Item (5) is new to our knowledge and needed to be confirmed by observations.

At an early stage of this work, the transport was calculated with 2-dimensional semi-Lagrangian scheme. In this case, a normal advective scheme was used in the vertical. The results of the 2-D scheme were different from those of the present study, especially vertical profiles in the lower stratosphere, and 2-D results produced larger vertical gradients, though the above results (1) through (5) do not change.

In this experiment, 12-hourly data were used. This data sampling interval might be too long. Currently, a calculation with 2-hourly data is underway.

Subgrid-scale diffusion is not included in the present study. It is important in the planetary boundary layer. If the subgrid-scale vertical diffusion is included, sharp vertical gradients near the surface in the SH would be reduced. This will be included in a future study. There are also plans to extend the calculation period to several years.

Acknowledgments

The authors would like to thank T. NAKAZAWA, S. AOKI, H. KIDA and J. HEINTZENBERG for their useful discussions and encouragement and K. SHIBATA for his contribution to developing the model. They are also grateful to two anonymous reviewers for comments on the first draft. Thanks are extended to D. V. BHASKAR RAO for reading the original manuscript.

Computations were carried out on the HITAC 810 computer at the Meteorological Research Institute.

References

AOKI, S. (1988): Nisanka tanso (Carbon dioxide). Nankyoku no Kagaku, 3. Kisho (Science in Antarctica, 3. Meteorology), ed. by Natl Inst. Polar Res. Tokyo, Kokon Shoin, 256–268.

CHIBA, M., KIDA, H., FUKUTANI, H., TANAKA, Y., KAWAHARA, M., YAMADA, S. and UENO, T. (1986): A simulation of seasonal change of the atmospheric general circulation with a low resolution spectral model. Part I: Calculated monthly mean fields. Pap. Meteorol. Geophys., **37**, 53–82.

HEINTZENBERG, J. (1989): Arctic haze: Air pollution in polar regions. Ambio, **18**, 50–55.

HEINTZENBERG, J. and BIGG, E. K. (1990): Tropospheric transport of trace substances in the southern hemisphere. Tellus, **42B**, 355–363.

HIROTA, M., CHUBACHI, S., MAKINO, Y. and MURAMATSU, H. (1984): Gas-chromatographic measurements of atmospheric CF_2Cl_2, $CFCl_3$ and N_2O in Antarctica. Mem. Natl Inst. Polar Res., Spec. Issue, **34**, 20–27.

HIROTA, M., MAKINO, Y., SHIOBARA, M., CHUBACHI, S. and MURAMATSU, H. (1985): Gas-chromatographic measurements of atmospheric CF_2Cl_2, $CFCl_3$ and N_2O from Tokyo to Syowa Station late in 1983, and at Syowa Station between February 1982 and January 1984. Mem. Natl Inst. Polar Res., Spec. Issue, **39**, 57–62.

HIROTA, M., MAKINO, Y. and MURAMATSU, H. (1986): The vertical distributions of atmospheric CF_2Cl_2, $CFCl_3$ and N_2O over Syowa Station in 1983. Mem. Natl Inst. Polar Res., Spec. Issue, **45**, 9–12.

HOFF, R. M. (1988): Vertical structure of arctic haze observed by lidar. Appl. Meteorol., **27**, 125–139.

KEELING, C. D., CARTER, A. F. and MOOK, W. G. (1984): Seasonal, latitudinal, and secular variations in the abundance and isotopic ratios of atmospheric CO_2, 2. Results from oceanographic cruises in the tropical Pacific Ocean. J. Geophys. Res., **89** (D3), 4615–4628.

KOMHYR, W. D., GAMMON, R. H., HARRIS, T. B., WATERMAN, L. S., CONWAY, T. J., TAYLOR, W. R. and THONING, K. W. (1985): Global atmospheric CO_2 distribution and variations from 1968–1982 NOAA/GMCC CO_2 flask sample data. J. Geophys. Res., **90** (D3), 5567–5596.

MAKINO, Y. (1988): Furon-gasu sonotano biryô seibun (Freon gas and other trace constituents). Nankyoku no Kagaku, 3. Kisho (Science in Antarctica, 3. Meteorology), ed. by Natl Inst. Polar Res. Tokyo, Kokon Shoin, 269–280.

NAKAZAWA, T., MURAYAMA, S., TANAKA, M., AOKI, S., KAWAGUCHI, S., FUKABORI, T., SHIOBARA, M. and MAKINO, Y. (1990): Nankyoku jôkû ni okeru taiki-chû no CO_2 nôdo (CO_2 concentration in the upper atmosphere above Antarctica). Dai-13-kai Kyokuiki Kisuiken Shinpojiumu Puroguramu·Kôen Yôshi (Program·Abstracts 13th Symp. Polar Meteorol. Glaciol.). Tokyo, Natl Inst. Polar Res., 67.

PEARMAN, G. I. and BEARDSMORE, D. J. (1984): Atmospheric carbon dioxide measurements in the Australian region: Ten years of aircraft data. Tellus, **36B**, 1–24.

PEARMAN, G. I. and GARRATT, J. R. (1973): Space and time variations of tropospheric carbon dioxide in the southern hemisphere. Tellus, **25**, 309–311.

RITCHIE, H. (1987): Semi-Lagrangian advection on a Gaussian grid. Mon. Weather Rev., **115**, 608–619.

SHIBATA, K. and CHIBA, M. (1990): A simulation of seasonal variation of the stratospheric circulation with a general circulation model. J. Meteorol. Soc. Jpn., **68**, 687–703.

TANAKA, M., NAKAZAWA, T. and AOKI, S. (1987): Seasonal and meridional variation of atmospheric carbon dioxide in the lower troposphere of the northern and southern hemispheres. Tellus, **39B**, 29–41.

WILLIAMSON, D. L. and RASCH, P. (1989): Two-dimensional semi-Lagrangian transport with shape-preserving interpolation. Mon. Weather Rev., **117**, 102–129.

WMO (1985): Halogenated species: Observations and interpretation. Atmospheric Ozone 1985. Geneva, WMO, 605–648 (WMO Global Ozone Research and Monitoring Project–Report No. 16).

YAMAZAKI, K. (1986): Preliminary calculation of trajectory analysis in the lower stratosphere of the southern hemisphere. Geophys. Res. Lett., **12**, 1312–1315.

YAMAZAKI, K. (1987): Transport characteristics in the troposphere and lower stratosphere of the southern hemisphere. Proc. NIPR Symp. Polar Meteorol. Glaciol., **1**, 39–53.

YAMAZAKI, K. (1989): Diffusion coefficients derived from the Lagrangian statistics. Proc. NIPR Symp. Polar Meteorol. Glaciol., **2**, 16–24.

(Received November 13, 1990; Revised manuscript received March 29, 1991)